conjugated with the synemin tail fragments. Other antibodies used for immunohistochemistry, immunoblotting, and immunoprecipitation were as follows: polyclonal and monoclonal anti-plectin antibody [(Hijikata et al., 2003) clone 7A8; Sigma-Aldrich], monoclonal and polyclonal anti-α-dystrobrevin antibody [Clone 23; BD Transduction Laboratories (Yoshida et al., 2000)], monoclonal anti-pan-actin antibody (C4; Novus Biological, Inc.), polyclonal anti-nonmuscle (β- and γ-) actin antibody (Cosmo Bio Co. Ltd.), monoclonal anti-integrin β1d antibody (clone 2B1; Chemicon International), monoclonal anti-α-actinin antibody (sarcomeric EA-53; Sigma-Aldrich), polyclonal and monoclonal anti-desmin antibody (Progen Biotechnik GmbH, DE-U-10; Sigma-Aldrich), monoclonal anti-Myc antibody (clone 9E10; Roche), monoclonal anti-vinculin antibody (clone hVin-1; Sigma-Aldrich), monoclonal anti-vimentin antibody (clone VIM13.2; Sigma-Aldrich), polyclonal anti-utrophin antibody (Imamura and Ozawa, 1998), monoclonal anti-dystrophin antibody (clone Dy8/6C5; Novocastra, clone mandy8; Sigma-Aldrich), monoclonal anti-developmental myosin heavy-chain antibody (clone RNMy2/9D2; Novocastra).

The secondary antibodies used in the present study were as follows: Alexa Fluor 488 goat anti-mouse IgG(H+L), Alexa Fluor 488 or Alexa Fluor 594 goat anti-rabbit IgG(H+L) (Invitrogen), peroxidase-conjugated goat anti-mouse IgG(H+L), goat anti-rabbit IgG(H+L) (Pierce), and rabbit anti-chicken IgY antibody (Promega), goat anti-rabbit IgG(H+L) conjugated to 5-nm gold particles (BioCell Research Laboratories).

Cell culture and transfection

C2C12 cells (2.0×10^5 cells) were cultured on collagen-coated Aclar coverslips within 35-mm dishes in growth medium (DMEM containing 20% FCS, 100 U/ml penicillin G and 100 μg/ml streptomycin). Plasmid DNA was prepared by subcloning exon 1 (Ex1), calponin homology domains (CHDα), plakin domain (PlD-M) cDNA fragments including Myc sequence into pZac expression vector (kindly provided by James M. Wilson. Plasmid DNA (4 μg) was transfected into the cells within each dish by using Lipofectamine™ 2000 (Invitrogen). After washing out plasmid DNA, the transfected cells were cultured in growth medium overnight, and then their differentiation was initiated by switching the medium to the DMEM medium containing 5% horse serum, 10 μg/ml insulin, and the antibiotics. After 2 or 3 days, C2C12 myotubes were fixed with chilled (–20°C) methanol and processed for immunostaining (Hijikata et al., 1997).

Immunofluorescence microscopy and immunoelectron microscopy

Cryosections of rat skeletal muscles (diaphragm and tibialis anterior) were prepared and immunostained as described previously (Hijikata et al., 1999). These sections were observed under a confocal scanning laser microscope (Fluoview FV1000, Olympus). For F-actin staining in C2C12 cells, Alexa Fluor 594-conjugated phallotoxins (Invitrogen) were utilized.

For immunoelectron microscopy, small bundles of muscle fibers were carefully teased from glycerinated muscle strips, chemically skinned with 50 μg/ml saponin in EGTA rigor solution, immunolabeled, processed for thin-section EM using tannic acid enhancement, and observed, as described previously (Hijikata et al., 2003).

Protein pull-down assay and immunoprecipitation

For pull-down assay, purified GST-synemin recombinant fragments were incubated with Myc-tagged PleN1 in the incubation buffer (50 mM HEPES pH 7.0, 10% glycerin, 1 mM DTT, 0.5% NP-40) for 3-4 hours at 4°C. The reaction mix was further incubated with anti-Myc mAb for 3-4 hours and then with protein L-agarose beads (Pierce) with rocking at 4°C overnight. The beads carrying the immune complexes were washed six times with the same buffer. The immune complexes were eluted by addition of SDS sample buffer. The Myc-tagged plectin recombinant fragments were also incubated with and pulled down by GST-synemin fragments Tail N1 and glutathione beads. Prior to the incubation, Myc-tagged plectin recombinant fragments were incubated with glutathione beads and precleared by centrifugation to remove contaminating plectin fragments still fused to GST. The glutathione beads carrying GST-synemin fragments associated with plectin fragments were washed six times with the incubation buffer and eluted with SDS sample buffer at 95°C.

For in vivo immunoprecipitation, light microsomes (LM), prepared from rat skeletal muscles according to the procedure described by Ohlendieck et al. (Ohlendieck et al., 1991), were lysed with solubilization buffer (150 mM NaCl, 1% Triton X-100, 0.1% SDS, 15% glycerol, 50 mM Tris-HCl pH 7.5) containing protease inhibitors (100 μg/ml PMSF, 2 μg/ml leupeptin). After centrifugation, the supernatant was precleared with protein G-Sepharose (Sigma-Aldrich). The precleared supernatant was incubated with either polyclonal anti-plectin or anti-synemin antibody and then with protein G-Sepharose overnight at 4°C. The beads carrying the immune complexes were washed three times with solubilization buffer, three times with solubilization buffer without SDS, and once with TBS (50 mM Tris-HCl, 150 mM NaCl, pH 7.5), followed by incubation with SDS sample buffer at 95°C.

Actin co-sedimentation assay

Actin was purified from rabbit skeletal muscle as described previously (Matsumura et al., 1983). The purity of actin was more than 97%, determined by SDS-PAGE. The actin was allowed to polymerize in the presence of recombinant plectin and synemin fragments in actin polymerization buffer (20 mM Tris-HCl pH 7.5, 2 mM $MgCl_2$, 100 mM KCl, 0.5 mM ATP, 0.1 mM β-mercaptoethanol) for 1 h at room temperature. Actin filaments with bound proteins were sedimented by centrifugation for 1 hour at 100,000 *g* and 20°C, and corresponding amounts of pellet and supernatant were analyzed by SDS-PAGE.

Blot overlay assay

Plectin PleN1 fragments (1 μg) were immobilized on nitrocellullose membranes, which were blocked in TBS containing 5% BSA and 0.2% Tween-20 for 5 hours at 4°C. Subsequently, membranes were overlaid and incubated with 3 μM actin or 1 μM α-dystrobrevin or 1 μM β-synemin or the mixture of the three proteins in 120 μl overlay buffer (20 mM HEPES pH 7.5, 150 mM NaCl, 2 mM $MgCl_2$, 1 mM DTT, and 3.5% BSA) overnight at 4°C. Bound proteins were detected by using the protein-specific antibody, HRP-conjugated secondary antibody and ECL system (GE Healthcare).

Densitometric analyses of overlay blots and immunoblots

Blot membranes treated with ECL solutions were scanned and evaluated using luminescent image analyzer LAS-3000 and Multi Gauge software (Fuji film). The mean value of spot intensities measured in the overlay with a single protein was calculated, and then each spot intensity was represented relative to this mean value by calculating the ratio of measured value per the mean value. Similarly, intensity of each band obtained in immunoblottings of control and dystrophin-deficient muscles was represented relative to the mean value of intensities measured in control muscles.

We thank J. M. Wilson (University of Pennsylvania) for providing pZac vector. This work was supported by a Research Grant (17A-10) for Nervous and Mental Disorders from the Ministry of Health, Labor and Welfare, and by the High-Tech Research Center Project for Private Universities (MEXT. HAITEKU, 2004-2008).

References

Ahn, A. H., Freener, C. A., Gussoni, E., Yoshida, M., Ozawa, E. and Kunkel, L. M. (1996). The three human syntrophin genes are expressed in diverse tissues, have distinct chromosomal locations, and each bind to dystrophin and its relatives. *J. Biol. Chem.* **271**, 2724-2730.

Andra, K., Lassmann, H., Bittner, R., Shorny, S., Fassler, R., Propst, F. and Wiche, G. (1997). Targeted inactivation of plectin reveals essential function in maintaining the integrity of skin, muscle, and heart cytoarchitecture. *Genes Dev.* **11**, 3143-3156.

Andra, K., Nikolic, B., Stocher, M., Drenckhahn, D. and Wiche, G. (1998). Not just scaffolding: plectin regulates actin dynamics in cultured cells. *Genes Dev.* **12**, 3442-3451.

Balogh, J., Li, Z., Paulin, D. and Arner, A. (2003). Lower active force generation and improved fatigue resistance in skeletal muscle from desmin deficient mice. *J. Muscle Res. Cell Motil.* **24**, 453-459.

Belkin, A. M., Zhidkova, N. I., Balzac, F., Altruda, F., Tomatis, D., Maier, A., Tarone, G., Koteliansky, V. E. and Burridge, K. (1996). Beta 1D integrin displaces the beta 1A isoform in striated muscles: localization at junctional structures and signaling potential in nonmuscle cells. *J. Cell Biol.* **132**, 211-226.

Bellin, R. M., Sernett, S. W., Becker, B., Ip, W., Huiatt, T. W. and Robson, R. M. (1999). Molecular characteristics and interactions of the intermediate filament protein synemin. Interactions with alpha-actinin may anchor synemin-containing heterofilaments. *J. Biol. Chem.* **274**, 29493-29499.

Bellin, R. M., Huiatt, T. W., Critchley, D. R. and Robson, R. M. (2001). Synemin may function to directly link muscle cell intermediate filaments to both myofibrillar Z-lines and costameres. *J. Biol. Chem.* **276**, 32330-32337.

Bhosle, R. C., Michele, D. E., Campbell, K. P., Li, Z. and Robson, R. M. (2006). Interactions of intermediate filament protein synemin with dystrophin and utrophin. *Biochem. Biophys. Res. Commun.* **346**, 768-777.

Bilak, S. R., Sernett, S. W., Bilak, M. M., Bellin, R. M., Stromer, M. H., Huiatt, T. W. and Robson, R. M. (1998). Properties of the novel intermediate filament protein synemin and its identification in mammalian muscle. *Arch. Biochem. Biophys.* **355**, 63-76.

Brenman, J. E., Chao, D. S., Gee, S. H., McGee, A. W., Craven, S. E., Santillano, D. R., Wu, Z., Huang, F., Xia, H., Peters, M. F. et al. (1996). Interaction of nitric oxide synthase with the postsynaptic density protein PSD-95 and alpha1-syntrophin mediated by PDZ domains. *Cell* **84**, 757-767.

Carlsson, L., Li, Z. L., Paulin, D., Price, M. G., Breckler, J., Robson, R. M., Wiche, G. and Thornell, L. E. (2000). Differences in the distribution of synemin, paranemin, and plectin in skeletal muscles of wild-type and desmin knock-out mice. *Histochem. Cell Biol.* **114**, 39-47.

Chan, Y., Anton-Lamprecht, I., Yu, Q. C., Jäckel, A., Zabel, B., Ernst, J. P. and Fuchs, E. (1994). A human keratin 14 "knockout": the absence of K14 leads to severe epidermolysis bullosa simplex and a function for an intermediate filament protein. *Genes Dev.* **8**, 2574-2587.

Craig, S. W. and Pardo, J. V. (1983). Gamma actin, spectrin, and intermediate filament proteins colocalize with vinculin at costameres, myofibril-to-sarcolemma attachment sites. *Cell Motil.* **3**, 449-462.

Dowling, J., Yu, Q. C. and Fuchs, E. (1996). Beta4 integrin is required for hemidesmosome formation, cell adhesion and cell survival. *J. Cell Biol.* **134**, 559-572.

Duclos, F., Straub, V., Moore, S. A., Venzke, D. P., Hrstka, R. F., Crosbie, R. H., Durbeej, M., Lebakken, C. S., Ettinger, A. J., van der Meulen, J. et al. (1998). Progressive muscular dystrophy in alpha-sarcoglycan-deficient mice. *J. Cell Biol.* **142**, 1461-1471.

Ervasti, J. M. and Campbell, K. P. (1993). A role for the dystrophin-glycoprotein complex as a transmembrane linker between laminin and actin. *J. Cell Biol.* **122**, 809-823.

Foisner, R., Leichtfried, F. E., Herrmann, H., Small, J. V., Lawson, D. and Wiche, G. (1988). Cytoskeleton-associated plectin: in situ localization, in vitro reconstitution, and binding to immobilized intermediate filament proteins. *J. Cell Biol.* **106**, 723-733.

Fontao, L., Geerts, D., Kuikman, I., Koster, J., Kramer, D. and Sonnenberg, A. (2001). The interaction of plectin with actin: evidence for cross-linking of actin filaments by dimerization of the actin-binding domain of plectin. *J. Cell Sci.* **114**, 2065-2076.

Fuchs, P., Zorer, M., Rezniczek, G. A., Spazierer, D., Oehler, S., Castanon, M. J., Hauptmann, R. and Wiche, G. (1999). Unusual 5′ transcript complexity of plectin isoforms: novel tissue-specific exons modulate actin binding activity. *Hum. Mol. Genet.* **8**, 2461-2472.

Fujikamki, N., Kano, Y. and Ishikawa, H. (1986). The association of intermediate filaments with the sarcolemma in skeletal muscle fibers. In Proc XIth Int Cong on Electron Microscopy, Kyoto, p2657-2658.

Gache, Y., Chavanas, S., Lacour, J. P., Wiche, G., Owaribe, K., Meneguzzi, G. and Ortonne, J. P. (1996). Defective expression of plectin/HD1 in epidermolysis bullosa simplex with muscular dystrophy. *J. Clin. Invest.* **97**, 2289-2298.

Geerts, D., Fontao, L., Nievers, M. G., Schaapveld, R. Q., Purkis, P. E., Wheeler, G. N., Lane, E. B., Leigh, I. M. and Sonnenberg, A. (1999). Binding of integrin alpha6beta4 to plectin prevents plectin association with F-actin but does not interfere with intermediate filament binding. *J. Cell Biol.* **147**, 417-434.

Grady, R. M., Grange, R. W., Lau, K. S., Maimone, M. M., Nichol, M. C., Stull, J. T. and Sanes, J. R. (1999). Role for alpha-dystrobrevin in the pathogenesis of dystrophin-dependent muscular dystrophies. *Nat. Cell Biol.* **1**, 215-220.

Granger, B. L. and Lazarides, E. (1980). Synemin: a new high molecular weight protein associated with desmin and vimentin filaments in muscle. *Cell* **22**, 727-738.

Hack, A. A., Ly, C. T., Jiang, F., Clendenin, C. J., Sigrist, K. S., Wollmann, R. L. and McNally, E. M. (1998). Gamma-sarcoglycan deficiency leads to muscle membrane defects and apoptosis independent of dystrophin. *J. Cell Biol.* **142**, 1279-1287.

Hack, A. A., Lam, M. Y., Cordier, L., Shorturma, D. I., Ly, C. T., Hadhazy, M. A., Hadhazy, M. R., Sweeney, H. L. and MaNally, E. M. (2000). Differential requirement for individual sarcoglycans and dystrophin in the assembly and function of the dystrophin-glycoprotein complex. *J. Cell Sci.* **113**, 2535-2544.

Hanft, L. M., Rybakova, I. N., Patel, J. R., Rafael-Fortney, J. A. and Ervasti, J. M. (2006). Cytoplasmic gamma-actin contributes to a compensatory remodeling response in dystrophin-deficient muscle. *Proc. Natl. Acad. Sci. USA* **103**, 5385-5390.

Hemken, P. M., Bellin, R. M., Sernett, S. W., Becker, B., Huiatt, T. W. and Robson, R. M. (1997). Molecular characteristics of the novel intermediate filament protein paranemin. Sequence reveals EAP-300 and IFAPa-400 are highly homologous to paranemin. *J. Biol. Chem.* **272**, 32489-32499.

Hieda, Y., Nishizawa, Y., Uematsu, J. and Owaribe, K. (1992). Identification of a new hemidesmosomal protein, HD1: a major, high molecular mass component of isolated hemidesmosomes. *J. Cell Biol.* **116**, 1497-1506.

Hijikata, T., Lin, Z. X., Holtzer, S., Choi, J., Sweeney, H. L. and Holtzer, H. (1997). Unanticipated temporal and spatial effects of sarcomeric alpha-actinin peptides expressed in PtK2 cells. *Cell Motil. Cytoskeleton* **38**, 54-74.

Hijikata, T., Murakami, T., Imamura, M., Fujimaki, N. and Ishikawa, H. (1999). Plectin is a linker of intermediate filaments to Z-discs in skeletal muscle fibers. *J. Cell Sci.* **112**, 867-876.

Hijikata, T., Murakami, T., Ishikawa, H. and Yorifuji, H. (2003). Plectin tethers desmin intermediate filaments onto subsarcolemmal dense plaques containing dystrophin and vinculin. *Histochem. Cell Biol.* **119**, 109-123.

Hirako, Y., Yamakawa, H., Tsujimura, Y., Nishizawa, Y., Okumura, M., Usukura, J., Matsumoto, H., Jackson, K. W., Owaribe, K. and Ohara, O. (2003). Characterization of mammalian synemin, an intermediate filament protein present in all four classes of muscle cells and some neuroglial cells: co-localization and interaction with type III intermediate filament proteins and keratins. *Cell Tissue Res.* **313**, 195-207.

Hodges, B. L., Hayashi, Y. K., Nonaka, I., Wang, W., Arahata, K. and Kaufman, S. J. (1997). Altered expression of the alpha7beta1 integrin in human and murine muscular dystrophies. *J. Cell Sci.* **110**, 2873-2881.

Hoffman, E. P., Brown, R. H., Jr and Kunkel, L. M. (1987). Dystrophin: the protein product of the Duchenne muscular dystrophy locus. *Cell* **51**, 919-928.

Huber, M., Floeth, M., Borradori, L., Schäcke, H., Rugg, E. L., Lane, E. B., Frenk, E., Hohl, D. and Bruckner-Tuderman, L. (2002). Deletion of the cytoplasmic domain of BP180/collagen XVII causes a phenotype with predominant features of epidermolysis bullosa simplex. *J. Invest. Dermatol.* **118**, 185-192.

Imamura, M. and Ozawa, E. (1998). Differential expression of dystrophin isoforms and utrophin during dibutyryl-cAMP-induced morphological differentiation of rat brain astrocytes. *Proc. Natl. Acad. Sci. USA* **95**, 6139-6144.

Law, D. J., Allen, D. L. and Tidball, J. G. (1994). Talin, vinculin and DRP (utrophin) concentrations are increased at mdx myotendinous junctions following onset of necrosis. *J. Cell Sci.* **107**, 1477-1483.

Lazarides, E. (1980). Intermediate filaments as mechanical integrators of cellular space. *Nature* **283**, 249-256.

Li, Z., Colucci-Guyon, E., Pincon-Raymond, M., Mericskay, M., Pournin, S., Paulin, D. and Babinet, C. (1996). Cardiovascular lesions and skeletal myopathy in mice lacking desmin. *Dev. Biol.* **175**, 362-366.

Li, Z., Mericskay, M., Agbulut, O., Butler-Browne, G., Carlsson, L., Thornell, L. E., Babinet, C. and Paulin, D. (1997). Desmin is essential for the tensile strength and integrity of myofibrils but not for myogenic commitment, differentiation, and fusion of skeletal muscle. *J. Cell Biol.* **139**, 129-144.

Litjens, S. H., de Pereda, J. M. and Sonnenberg, A. (2006). Current insights into the formation and breakdown of hemidesmosomes. *Trends Cell Biol.* **16**, 376-383.

Lunter, P. C. and Wiche, G. (2002). Direct binding of plectin to Fer kinase and negative regulation of its catalytic activity. *Biochem. Biophys. Res. Commun.* **296**, 904-910.

Matsumura, F., Yamashiro-Matsumura, S. and Lin, J. J. (1983). Isolation and characterization of tropomyosin-containing microfilaments from cultured cells. *J. Biol. Chem.* **258**, 6636-6664.

Mayer, U., Saher, G., Fässler, R., Bornemann, A., Echtermeyer, F., von der Mark, H., Miosge, N., Pöschl, E. and von der Mark, K. (1997). Absence of integrin alpha 7 causes a novel form of muscular dystrophy. *Nat. Genet.* **17**, 318-323.

McMillan, J. R., Akiyama, M., Rouan, F., Mellerio, J. E., Lane, E. B., Leigh, I. M., Owaribe, K., Wiche, G., Fujii, N., Uitto, J. et al. (2007). Plectin defects in epidermolysis bullosa simplex with muscular dystrophy. *Muscle Nerve* **35**, 24-35.

Mizuno, Y., Thompson, T. G., Guyon, J. R., Lidov, H. G., Brosius, M., Imamura, M., Ozawa, E., Watkins, S. C. and Kunkel, L. M. (2001). Desmuslin, an intermediate filament protein that interacts with alpha-dystrobrevin and desmin. *Proc. Natl. Acad. Sci. USA* **98**, 6156-6161.

Mizuno, Y., Guyon, J. R., Watkins, S. C., Mizushima, K., Sasaoka, T., Imamura, M., Kunkel, L. M. and Okamoto, K. (2004). Beta-synemin localizes to regions of high stress in human skeletal myofibers. *Muscle Nerve* **30**, 337-346.

Nikolic, B., Mac Nulty, E., Mir, B. and Wiche, G. (1996). Basic amino acid residue cluster within nuclear targeting sequence motif is essential for cytoplasmic plectin-vimentin network junctions. *J. Cell Biol.* **134**, 1455-1467.

Ohlendieck, K., Ervasti, J. M., Snook, J. B. and Campbell, K. P. (1991). Dystrophin-glycoprotein complex is highly enriched in isolated skeletal muscle sarcolemma. *J. Cell Biol.* **112**, 135-148.

Ozawa, E. (2006). The functional biology of dystrophin: structural components and the pathogenesis of Duchenne muscular dystrophy. In *Duchenne Muscular Dystrophy Advances in Therapeutics* (ed. J. S. Chamberlain and T. A. Rando), pp. 21-53. New York, London: Taylor & Francis Group.

Ozawa, E., Noguchi, S., Mizuno, Y., Hagiwara, Y. and Yoshida, M. (1998). From dystrophinopathy to sarcoglycanopathy: evolution of a concept of muscular dystrophy. *Muscle Nerve* **21**, 421-438.

Ozawa, E., Imamura, M., Noguchi, S. and Yoshida, M. (2000). Dystrophinopathy and sarcoglycanopathy. *NeuroScience News* **3**, 13-19.

Peters, M. F., Sadoulet-Puccio, H. M., Grady, M. R., Kramarcy, N. R., Kunkel, L. M., Sanes, J. R., Sealock, R. and Froehner, S. C. (1998). Differential membrane localization and intermolecular associations of alpha-dystrobrevin isoforms in skeletal muscle. *J. Cell Biol.* **142**, 1269-1278.

Pham, C. G., Harpf, A. E., Keller, R. S., Vu, H. T., Shai, S. Y., Loftus, J. C. and Ross, R. S. (2000). Striated muscle-specific beta(1D)-integrin and FAK are involved in cardiac myocyte hypertrophic response pathway. *Am. J. Physiol. Heart Circ. Physiol.* **279**, H2916-H2926.

Price, M. G. and Lazarides, E. (1983). Expression of intermediate filament-associated proteins paranemin and synemin in chicken development. *J. Cell Biol.* **97**, 1860-1874.

Pulkkinen, L., Kimonis, V. E., Xu, Y., Spanou, E. N., McLean, W. H. and Uitto, J. (1997). Homozygous alpha6 integrin mutation in junctional epidermolysis bullosa with congenital duodenal atresia. *Hum. Mol. Genet.* **6**, 669-674.

Reipert, S., Steinbock, F., Fischer, I., Bittner, R. E., Zeold, A. and Wiche, G. (1999). Association of mitochondria with plectin and desmin intermediate filaments in striated muscle. *Exp. Cell Res.* **252**, 479-491.

Rezniczek, G. A., de Pereda, J. M., Reipert, S. and Wiche, G. (1998). Linking integrin alpha6beta4-based cell adhesion to the intermediate filament cytoskeleton: direct interaction between the beta4 subunit and plectin at multiple molecular sites. *J. Cell Biol.* **141**, 209-225.

Rezniczek, G. A., Abrahamsberg, C., Fuchs, P., Spazierer, D. and Wiche, G. (2003). Plectin 5′-transcript diversity: short alternative sequences determine stability of gene products, initiation of translation and subcellular localization of isoforms. *Hum. Mol. Genet.* **12**, 3181-3194.

Rezniczek, G. A., Konieczny, P., Nikolic, B., Reipert, S., Schneller, D., Abrahamsberg, C., Davies, K. E., Winder, S. J. and Wiche, G. (2007). Plectin 1f scaffolding at the sarcolemma of dystrophic (mdx) muscle fibers through multiple interactions with beta-dystroglycan. *J. Cell Biol.* **176**, 965-977.

Rybakova, I. N., Patel, J. R. and Ervasti, J. M. (2000). The dystrophin complex forms a mechanically strong link between the sarcolemma and costameric actin. *J. Cell Biol.* **150**, 1209-1214.

Sadoulet-Puccio, H. M., Rajala, M. and Kunkel, L. M. (1997). Dystrobrevin and dystrophin: an interaction through coiled-coil motifs. *Proc. Natl. Acad. Sci. USA* **94**, 12413-12418.

Sam, M., Shah, S., Friden, J., Milner, D. J., Capetanaki, Y. and Lieber, R. L. (2000). Desmin knockout muscles generate lower stress and are less vulnerable to injury compared with wild-type muscles. *Am. J. Physiol. Cell Physiol.* **279**, C1116-C1122.

Schröder, R., Mundegar, R. R., Treusch, M., Schlegel, U., Blumcke, I., Owaribe, K. and Magin, T. M. (1997). Altered distribution of plectin/HD1 in dystrophinopathies. *Eur. J. Cell Biol.* **74**, 165-171.

Schröder, R., Warlo, I., Herrmann, H., van der Ven, P. F., Klasen, C., Blümcke, I., Mundegar, R. R., Fürst, D. O., Goebel, H. H. and Magin, T. M. (1999). Immunogold EM reveals a close association of plectin and the desmin cytoskeleton in human skeletal muscle. *Eur. J. Cell Biol.* **78**, 288-295.

Schröder, R., Pacholsky, D., Reimann, J., Matten, J., Wiche, G., Furst, D. O. and van der Ven, P. F. (2002). Primary longitudinal adhesion structures: plectin-containing precursors of costameres in differentiating human skeletal muscle cells. *Histochem. Cell Biol.* **118**, 301-310.

Schweitzer, S. C., Klymkowsky, M. W., Bellin, R. M., Robson, R. M., Capetanaki, Y. and Evans, R. M. (2001). Paranemin and the organization of desmin filament networks. *J. Cell Sci.* **114**, 1079-1089.

Sevcik, J., Urbániková, L., Kost'an, J., Janda, L. and Wiche, G. (2004). Actin-binding domain of mouse plectin. Crystal structure and binding to vimentin. *Eur. J. Biochem.* **271**, 1873-1884.

Straub, V. and Campbell, K. P. (1997). Muscular dystrophies and the dystrophin-glycoprotein complex. *Curr. Opin. Neurol.* **10**, 168-175.

Titeux, M., Brocheriou, V., Xue, Z., Gao, J., Pellissier, J. F., Guicheney, P., Paulin, D. and Li, Z. (2001). Human synemin gene generates splice variants encoding two distinct intermediate filament proteins. *Eur. J. Biochem.* **268**, 6435-6449.

Tokuyasu, K. T., Dutton, A. H. and Singer, S. J. (1983). Immunoelectron microscopic studies of desmin (skeletin) localization and intermediate filament organization in chicken skeletal muscle. *J. Cell Biol.* **96**, 1727-1735.

van der Neut, R., Krimpenfort, P., Calafat, J., Niessen, C. M. and Sonnenberg, A. (1996). Epithelial detachment due to absence of hemidesmosomes in integrin beta 4 null mice. *Nat. Genet.* **13**, 366-369.

Wilhelmsen, K., Litjens, S. H., Kuikman, I., Tshimbalanga, N., Janssen, H., van den Bout, I., Raymond, K. and Sonnenberg, A. (2005). Nesprin-3, a novel outer nuclear membrane protein, associates with the cytoskeletal linker protein plectin. *J. Cell Biol.* **171**, 799-810.

Witt, S., Zieseniss, A., Fock, U., Jockusch, B. M. and Illenberger, S. (2004). Comparative biochemical analysis suggests that vinculin and metavinculin cooperate in muscular adhesion sites. *J. Biol. Chem.* **279**, 31533-31543.

Yoshida, M., Suzuki, A., Yamamoto, H., Noguchi, S., Mizuno, Y. and Ozawa, E. (1994). Dissociation of the complex of dystrophin and its associated proteins into several unique groups by n-octyl beta-D-glucoside. *Eur. J. Biochem.* **222**, 1055-1061.

Yoshida, M., Hama, H., Ishikawa-Sakurai, M., Imamura, M., Mizuno, Y., Araishi, K., Wakabayashi-Takai, E., Noguchi, S., Sasaoka, T. and Ozawa, E. (2000). Biochemical evidence for association of dystrobrevin with the sarcoglycan-sarcospan complex as a basis for understanding sarcoglycanopathy. *Hum. Mol. Genet.* **9**, 1033-1040.

HUMAN GENE THERAPY 19:719–730 (July 2008)

DOI: 10.1089/hum.2007.184

Recombinant Adeno-Associated Virus Type 8-Mediated Extensive Therapeutic Gene Delivery into Skeletal Muscle of α-Sarcoglycan-Deficient Mice

Akiyo Nishiyama,[1] Beryl Nyamekye Ampong,[1] Sachiko Ohshima,[1] Jin-Hong Shin,[1] Hiroyuki Nakai,[2] Michihiro Imamura,[1] Yuko Miyagoe-Suzuki,[1] Takashi Okada,[1] and Shin'ichi Takeda[1]

Abstract

Autosomal recessive limb-girdle muscular dystrophy type 2D (LGMD 2D) is caused by mutations in the α-sarcoglycan gene (α-SG). The absence of α-SG results in the loss of the SG complex at the sarcolemma and compromises the integrity of the sarcolemma. To establish a method for recombinant adeno-associated virus (rAAV)-mediated α-SG gene therapy into α-SG-deficient muscle, we constructed rAAV serotypes 2 and 8 expressing the human α-SG gene under the control of the ubiquitous cytomegalovirus promoter (rAAV2-α-SG and rAAV8-α-SG). We compared the transduction profiles and evaluated the therapeutic effects of a single intramuscular injection of rAAVs into α-SG-deficient ($Sgca^{-/-}$) mice. Four weeks after rAAV2 injection into the tibialis anterior (TA) muscle of 10-day-old $Sgca^{-/-}$ mice, transduction of the α-SG gene was localized to a limited area of the TA muscle. On the other hand, rAAV8-mediated α-SG expression was widely distributed in the hind limb muscle, and persisted for 7 months without inducing cytotoxic and immunological reactions, with a reversal of the muscle pathology and improvement in the contractile force of the $Sgca^{-/-}$ muscle. This extensive rAAV8-mediated α-SG transduction in LGMD 2D model animals paves the way for future clinical application.

Introduction

LIMB-GIRDLE MUSCULAR DYSTROPHY TYPE 2D (LGMD 2D) is caused by mutations in the α-sarcoglycan (α-SG) gene, and is the most frequent cause of the autosomal recessive LGMD. LGMD 2D patients have the clinical characteristics of progressive muscle necrosis in the proximal limb muscles (Eymard *et al.*, 1997). Sarcoglycans (SGs) are essential constituents of the dystrophin-associated protein (DAP) complex, which consists of several membrane-spanning and cytoplasmic proteins, including dystroglycans (α and β), SGs (α, β, γ, and δ), sarcospan, syntrophins (α_1, β_1, and β_2), and dystrobrevins that directly or indirectly associate with dystrophin (Ervasti *et al.*, 1990; Yoshida and Ozawa, 1990; Iwata *et al.*, 1993). A defect in any one of the four SGs can disrupt the entire SG complex. Mutations in four genes encoding α-, β-, γ-, and δ-SG are responsible for autosomal recessive LGMD 2D, 2E, 2C and 2F, respectively (Ervasti *et al.*, 1990; Bonnemann *et al.*, 1995; Noguchi *et al.*, 1995; Nigro *et al.*, 1996; Eymard *et al.*, 1997; Fanin *et al.*, 1997).

Many *in vivo* studies have demonstrated that recombinant adeno-associated virus (rAAV) packaged in various serotypes of AAV capsids exhibits serotype-specific tissue or cell tropism with different transduction efficiencies (Fisher *et al.*, 1997; Greelish *et al.*, 1999; Gao *et al.*, 2002, 2004; Wang *et al.*, 2005). rAAV has been shown to mediate long-term transgene expression in many tissues without evoking severe immune reactions. Some rAAVs efficiently transduce skeletal muscle (Kessler *et al.*, 1996; Xiao *et al.*, 1996; Fisher *et al.*, 1997). rAAV serotype 2 (rAAV2)-mediated muscle gene therapy is a promising approach, but it is effective only locally. In contrast, rAAV serotype 8 (rAAV8)-mediated gene transfer is capable of crossing capillary blood vessels to achieve systemic gene delivery, and effectively transduces genes into cardiac and skeletal muscle (Wang *et al.*, 2005). Therefore, rAAV8 is a good candidate for a therapeutic tool.

To assess the efficacy and therapeutic potential of rAAV8 for LGMD 2D, we directly injected rAAV2-α-SG and rAAV8-α-SG into the tibialis anterior (TA) muscles of 10-day-old α-SG-deficient mice (neonatal $Sgca^{-/-}$ mice). Our data suggested not

[1]Department of Molecular Therapy, National Institute of Neuroscience, National Center of Neurology and Psychiatry, Tokyo 187-8502, Japan.
[2]Department of Molecular Genetics and Biochemistry, University of Pittsburgh School of Medicine, Pittsburgh, PA 15261.

only the extensive expression of α-SG in Sgca$^{-/-}$ skeletal muscle, but also a robust level of expression of α-SG at the sarcolemma after a single intramuscular injection of rAAV8-α-SG. In addition, rAAV8-α-SG effectively transduced the cardiac muscle of 7-week-old Sgca$^{-/-}$ mice (adult Sgca$^{-/-}$ mice). Most importantly, 7 months after the injection of rAAV8-α-SG into neonatal Sgca$^{-/-}$ mice, expression of α-SG and improvement of sarcolemmal function were sustained, without inducing cytotoxic and immunological reactions. Thus, the AAV8 vector is a promising tool for gene therapy of LGMD 2D.

Materials and Methods

Recombinant AAV production

The full-length human α-SG cDNA was amplified from a skeletal muscle single-strand cDNA library (Human Skeletal Muscle Marathon-Ready cDNA; Clontech, Palo Alto, CA) by polymerase chain reaction (PCR) with the following set of oligonucleotide primers: 5′-CTCTGTCACTCACCGGG-3′ (nucleotide positions 2–18) and 5′-AGGATGAAGTC-AGGGCTGGAC-3′ (nucleotide positions 1223–1243) (McNally *et al.*, 1994). The amplification was carried out with LA-Taq polymerase (TaKaRa Bio, Shiga, Japan) for 30 cycles, with each cycle consisting of 94°C for 30 sec and 60°C for 2 min. The PCR products were then cloned into a TA cloning vector (Invitrogen, Carlsbad, CA), and sequenced with an ABI310 sequencer (Applied Biosystems, Foster City, CA). α-SG cDNA was then cloned into an AAV serotype 2 vector plasmid (Xiao *et al.*, 1998; Yuasa *et al.*, 2002) including the cytomegalovirus (CMV) promoter, splicing donor/acceptor (SD/SA) sites derived from the simian virus 40 (SV40), an SV40 poly(A) signal, inverted terminal repeat (ITR) of the AAV2 viral genome, and 2.0 kb of λ DNA, which served as a stuffer (depicted in Fig. 1A).

The vector genome was packaged in the AAV2 capsid or pseudotyped into the AAV8 capsid by triple transfection of

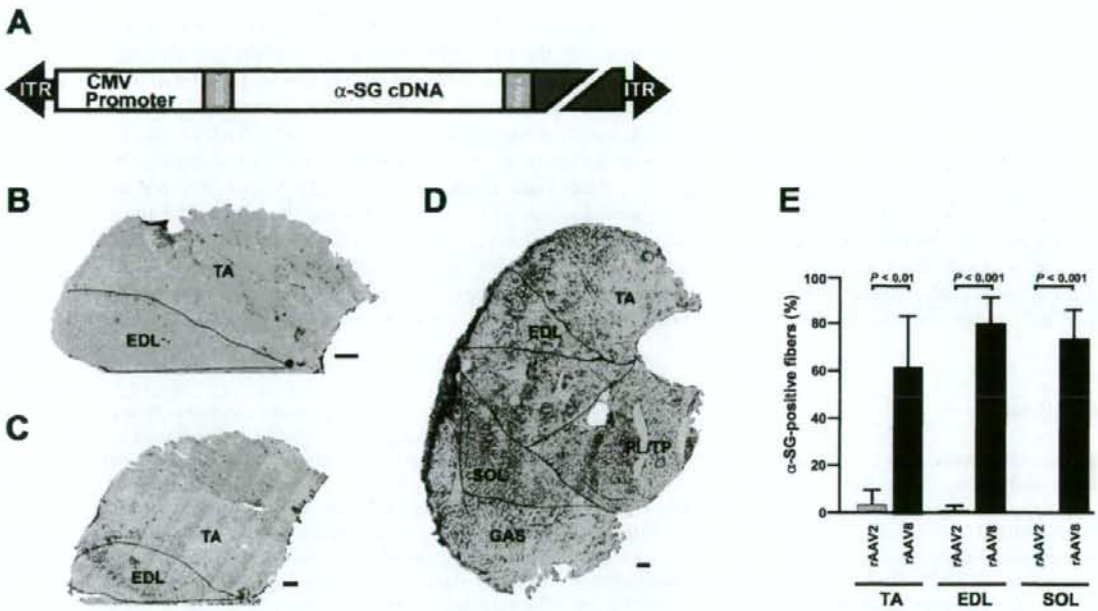

FIG. 1. Widespread expression of α-SG in hind limb muscles after a single injection of rAAV2-α-SG or rAAV8-α-SG into the tibialis anterior (TA) muscles of 10-day-old α-SG-deficient mice. (**A**) Genomic structure of rAAV used in this study. Human α-SG cDNA (1.2 kb) was inserted downstream of the CMV promoter. ITR, inverted terminal repeat from AAV2 genome; SD/SA, splicing donor/acceptor sites derived from SV40 intron; poly(A), a polyadenylation signal from SV40. The large shaded box represents a stuffer sequence derived from λ DNA. (**B–D**) Right TA muscles of neonatal Sgca$^{-/-}$ mice were injected with 1×10^{11} VG of rAAV2-α-SG (**C**) or rAAV8-α-SG (**D**). Four weeks after rAAV injection, the hind limb muscles of Sgca$^{-/-}$ mice were immunolabeled with a rabbit polyclonal antibody to α-SG. Hind limb muscles included the TA, extensor digitorum longus (EDL), plantaris (PL)/tibialis posterior (TP), soleus (SOL), and gastrocnemius (GAS) muscles. The TA and EDL muscles of Sgca$^{-/-}$ mice are shown as negative controls (**B**). Note that α-SG is expressed not only in rAAV8-injected TA muscle, but also in all hind limb muscles after direct injection of rAAV8-α-SG into the right TA muscle (**D**). Scale bars (**B–D**): 500 μm. (**E**) Percentages of α-SG-positive myofibers in TA, EDL, and SOL muscles after injection of rAAV2-α-SG (shaded columns) and rAAV8-α-SG (solid columns) injection into TA muscles of Sgca$^{-/-}$ mice. The right TA muscles of neonatal Sgca$^{-/-}$ mice were transduced with 1×10^{11} VG of rAAV2-α-SG or rAAV8-α-SG. Four weeks after rAAV injection, the hind limb muscles of Sgca$^{-/-}$ mice were immunolabeled with the α-SG antibody and then counterstained with hematoxylin and eosin. Hind limb muscles include the TA, EDL, and SOL muscles. The percentage of α-SG-positive myofibers was calculated on the basis of more than 200 total myofibers in cross-sections from three animals for each group. *p* Values are indicated and show statistical significance between Sgca$^{-/-}$ mice and rAAV8-injected Sgca$^{-/-}$ mice ($p < 0.01$ for TA, $p < 0.001$ for EDL, and $p < 0.001$ for SOL).

the AAV vector plasmid, AAV helper plasmid (p5E18-VD2/8) (Wang *et al.*, 2005), and adenovirus helper plasmid (XX6) (Xiao *et al.*, 1998) at a molecular ratio of 1:1:1 in 293 cells, using the calcium phosphate coprecipitation method (Wigler *et al.*, 1980). All the vectors were then purified by two cycles of cesium chloride gradient centrifugation, and concentrated as described by Burton and coworkers (1999). The final viral preparations were kept in phosphate-buffered saline. Physical particle titers were determined by a quantitative dot-blot assay.

Administration of rAAV vectors to murine skeletal muscle

All animal-handling procedures were done in accordance with a protocol approved by the committee of the National Institute of Neuroscience (National Center of Neurology and Psychiatry, Kodaira, Japan). Wild-type ($Sgca^{+/+}$) and $Sgca^{-/-}$ mice (Burnham Institute, La Jolla, CA) were used. The TA muscles of 10-day-old (neonate) and 7-week-old (adult) $Sgca^{-/-}$ mice were transduced with 1×10^{11} vector genomes (VG) (10 μl) and 5×10^{11} VG (50 μl), respectively, of rAAV2- or rAAV8-α-SG, using 29-gauge needles.

Transgene expression analyses

Histological and immunohistochemical analyses were performed as described (Imamura *et al.*, 2000; Yuasa *et al.*, 2002). Cryosections (6 μm thick) were prepared from frozen muscle.

For colorimetric immunodetection of α-SG, blocked cryosections were incubated with a 1:1000 dilution of rabbit polyclonal anti-α-SG (Araishi *et al.*, 1999) for 1 hr at room temperature. The signal was visualized with a VECTASTAIN ABC kit (Vector Laboratories, Burlingame, CA) and then counterstained with hematoxylin and eosin (H&E). Stained sections were photographed with a light microscope (Leica, Heidelberg, Germany) using DP70 image scanning software (Olympus, Tokyo, Japan).

For fluorescence immunohistochemical detection of SGs, cryosections were fixed by immersion in cold acetone at –20°C for 5 min. After blocking with 2% casein in Tris-buffered saline (TBS, pH 7.4) at room temperature for 1 hr, α-SG was detected with rabbit polyclonal anti-α-SG (1:1000 dilution) (Araishi *et al.*, 1999). β-, γ-, and δ-SGs were detected with mouse monoclonal anti-β-SG (NCL-b-SARC, 1:50 dilution; Novocastra Laboratories, Newcastle-upon-Tyne, UK), anti-γ-SG (1:50 dilution), and anti-δ-SG (DSG-1; 1:50 dilution), respectively, after blocking with an M.O.M. kit (Vector Laboratories). Mouse monoclonal antibodies against γ-SG and δ-SG (DSG-1) were generated in our laboratory (Yamamoto *et al.*, 1994; Noguchi *et al.*, 1999). The signal was visualized with Alexa 488-conjugated anti-rabbit and anti-mouse IgG antibodies (Invitrogen Molecular Probes, Eugene, OR). Fluorescence signals were observed with a confocal laser-scanning microscope (Leica TCS SP; Leica).

Sodium dodecyl sulfate–polyacrylamide gel electrophoresis (SDS–PAGE) and protein transfer to a polyvinylidene di-

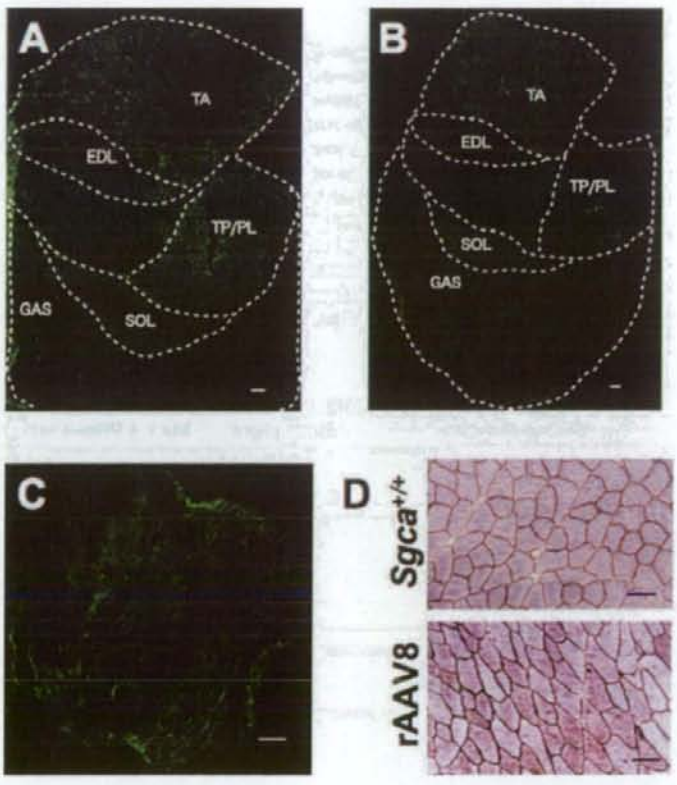

FIG. 2. Extensive α-SG expression after injection of rAAV8-α-SG into TA muscles of 7-week-old α-SG-deficient mice. Right TA muscles of adult $Sgca^{-/-}$ or $Sgca^{+/+}$ mice were transduced with 5×10^{11} VG of rAAV8-α-SG. Four weeks after rAAV8 injection, a cross-section of the right hind limb muscles (rAAV8-injected) (**A**), left contralateral hind limb muscles (**B**), and cardiac apex (**C**) were labeled by indirect immunofluorescence, using α-SG antibody (green). Scale bars: (**A** and **B**) 500 μm; (**C**) 100 μm. Note the widespread expression of α-SG in the hind limb muscles and cardiac muscle of rAAV8-α-SG-injected mice. (**D**) Cross-sections of TA muscle from $Sgca^{+/+}$ and rAAV8-injected $Sgca^{+/+}$ (rAAV8) mice were immunolabeled with α-SG antibody and counterstained with hematoxylin and eosin. Overexpression of α-SG caused no cytotoxic reactions in $Sgca^{+/+}$ muscle. Scale bars (**D**): 50 μm.

fluoride (PVDF) membrane were performed as described by Laemmli (1970) and Kyhse-Andersen (1984), respectively. Protein concentrations were determined with a protein assay kit (Bio-Rad, Hercules, CA) with bovine serum albumin as a standard.

Transgene copy number analyses

Cryosections of mouse hind limb muscle were collected for vector copy number analysis by quantitative PCR. After DNA extraction by successive treatments with RNase and proteinase K, viral genomes were quantified by a real-time PCR assay using SYBR *Premix Ex Taq* (TaKaRa Bio). The real-time PCR was carried out for 40 cycles, with each cycle consisting of 95°C for 5 sec, 60°C for 10 sec, 72°C for 10 sec, and 75°C for 10 sec. Oligonucleotide primers for this assay were 5′-CTCTAGAGGATCCGGTACTCGAGGAAC-3′ (SD/SA sites) and 5′-AGAGGAGTCCAGAAGAGTGTCTCAGCC-3′ (human α-SG gene) for the α-SG gene in the rAAV2 genome and 5′-TGCCATGAGCAGCCCATTTTG-3′ and 5′-ATAACATCGCGGTGGCTCAGG-3′ for the slug promoter. The slug promoter was used for normalization of data across samples.

Analysis of toxicity

Blood was obtained from a murine heart. Serum alanine aminotransferase, γ-glutamyl transpeptidase, albumin, and total protein concentration were determined with a Fuji Dri-Chem slide system (Fujifilm, Tokyo, Japan).

Muscle physiological function

TA and extensor digitorum longus (EDL) muscles were exposed by removal of overlying connective tissue (Xiao *et al.*, 2000; Yoshimura *et al.*, 2004; Imamura *et al.*, 2005). Both tendons of the TA and EDL muscles were cut from their insertions and secured with 5-0 silk sutures. Muscles were mounted in a vertical tissue chamber containing physiological salt solution (150 m*M* NaCl, 4 m*M* KCl, 1.8 m*M* $CaCl_2$, 1 m*M* $MgCl_2$, 5 m*M* HEPES, 5.6 m*M* glucose [pH 7.4], and 0.02 m*M* D-tubocurarine) maintained at 37°C with continuous aeration. The chamber was connected to a force transducer (UL-10GR; Minerva, Nagano, Japan) and a length servosystem (MM-3; Narishige, Tokyo, Japan). Electrical stimulation (SEN3301; Nihon Kohden, Tokyo, Japan) was delivered through a pair of platinum wires placed on both sides of the muscle. The muscle fiber length was adjusted incrementally with a micropositioner until peak isometric twitch force responses were obtained (i.e., optimal fiber length L_o). L_o was measured with a microcaliper. Maximal tetanic force (P_o) was induced by stimulation frequencies of 125 pulses per second, delivered in trains of 500-msec duration with 2-min intervals between each train. The muscle was weighed, rapidly frozen in liquid nitrogen-cooled isopentane, and stored at −80°C for further analysis. All forces were normalized to the physiological cross-section area (CSA), which was estimated on the basis of the following formula: muscle wet weight (in mg)/[L_o (in mm) × 1.06 (in mg/mm^3)]. The estimated CSA was used to determine specific tetanic (P_o/CSA) force of the muscle. Data are presented as means ± SE. Differences between groups were assessed by Student *t* test.

Exercise tolerance tests

Mice were subjected to an exhaustion treadmill test (Mourkioti *et al.*, 2006). Each mouse was placed on the belt of a four-lane motorized treadmill (MK-680; Muromachi Kikai, Tokyo, Japan) supplied with shocker plates. The treadmill was run at an inclination of 7 degrees at 5 m/min for 5 min, after which the speed was increased by 1 m/min every minute. The test was terminated when the mouse remained on the shocker plate for more than 20 sec without attempting to reengage the treadmill, and the time to exhaustion was determined.

Results

Expression of α-SG after injection of rAAV2- or rAAV8-α-SG into TA muscles of neonatal α-SG-deficient mice

We constructed rAAV2- and rAAV8-α-SG expressing human α-SG cDNA under the control of the ubiquitous CMV promoter, and injected 1×10^{11} VG into the right TA muscle of neonatal Sgca$^{-/-}$ mice (Fig. 1A). Neonatal Sgca$^{-/-}$ mice showed no obvious dystrophic changes, whereas adult (>4 weeks old) Sgca$^{-/-}$ skeletal muscles showed active cycles of the degeneration–regeneration process. In the hind limb muscles of 5-week-old Sgca$^{-/-}$ mice, α-SG-positive

TABLE 1. EFFECT OF rAAV2- AND rAAV8-α-SARCOGLYCAN ADMINISTRATION ON THE LIVER FUNCTION OF ADULT Sgca$^{-/-}$ MICE 4 WEEKS AFTER INJECTION[a,b]

	Number of mice	*ALT (U/liter)*	*γ-GTP (U/liter)*	*ALB (g/dl)*	*TP (g/dl)*
Sgca$^{+/+}$	3	26.67 ± 8.50[c]	<10	2.43 ± 0.21	4.80 ± 0.20
Sgca$^{-/-}$	3	145.33 ± 22.22	<10	2.33 ± 0.23	4.60 ± 0.42
rAAV2-injected Sgca$^{-/-}$	3	149 ± 9[d]	<10	2.10 ± 0.44	4.00 ± 0.53
rAAV8-injected Sgca$^{-/-}$	3	124 ± 15.10[e]	<10	2.03 ± 0.25	4.60 ± 0.89

Abbreviations: ALT/GPT, alanine aminotransferase/glutamic pyruvic transaminase; γ-GTP, γ-glutamyl transpeptidase; ALB, albumin; TP, total protein.

[a]Data represent means ± SE.

[b]The *p* values indicate statistical significance. Significant differences from the ALT/GPT level of Sgca$^{-/-}$ mice are indicated.

[c]$p < 0.001$.

[d]$p = 0.797$.

[e]$p = 0.229$.

fibers were not observed and the active cycle of muscle degeneration–regeneration was present (Fig. 1B). Four weeks after a single intramuscular injection of rAAV2-α-SG, α-SG was expressed only in a limited area of rAAV2-injected TA muscle (Fig. 1C and E). Analysis of TA muscle showed that less than 10% of muscle fibers were α-SG positive ($p < 0.01$; Fig. 1E).

In contrast, after rAAV8-α-SG injection, α-SG-positive fibers were widely spread in rAAV8-injected hind limb muscles, including the TA, extensor digitorum longus (EDL), soleus (SOL), gastrocnemius (GAS), and plantaris (PL)/tibialis posterior (TP) muscles (Fig. 1D). Analysis of the TA, EDL, and SOL muscles showed 62.3 ± 20.2, 79.5 ± 11.0, and 74.2 ± 11.2% α-SG-positive fibers, respectively ($p < 0.01$, $p < 0.001$, and $p < 0.001$; Fig. 1E). The expression of α-SG in rAAV8-α-SG-injected TA muscle and surrounding muscles persisted more than 7 months (data not shown).

Expression of α-SG after injection of rAAV2-α-SG or rAAV8-α-SG into TA muscles of adult α-SG-deficient mice

Adult Sgca$^{-/-}$ mice (>4 weeks old) showed active cycles of the degeneration–regeneration process and had a mature immune system. To investigate whether injection of rAAV2-α-SG or rAAV8-α-SG could induce stable expression of α-SG in adult Sgca$^{-/-}$ skeletal muscle without cytotoxicity and immune response, we injected 5×10^{11} VG of rAAV2-α-SG or rAAV8-α-SG into the right TA muscles of adult Sgca$^{-/-}$ mice. Four weeks after rAAV2-α-SG injection, we did not observe α-SG-positive fibers in the right TA muscle (data not shown). rAAV2-α-SG-injected TA muscles showed the degeneration–regeneration process. In contrast, after rAAV8-α-SG injection, we observed numerous α-SG-positive fibers in the entirety of rAAV8-injected hind limb muscles (Fig. 2A). Moreover, α-SG-positive fibers were detected even in contralateral hind limb muscles and cardiac muscle (Fig. 2B and C). In particular, when rAAV8-α-SG was injected into the TA muscle of Sgca$^{+/+}$ mice, we observed no pathological changes in the injected hind limb muscles 4 weeks after injection (Fig. 2D). No signs of tissue damage were found in regions where α-SG was detected after injection of rAAV8-α-SG. α-SG-positive myofibers retained normal morphology up to 4 weeks after injection. In addition, to examine whether rAAV2-α-SG and rAAV8-α-SG administration affect liver function, we measured the serum level of liver-related isozymes including alanine aminotransferase (ALT), γ-glu-

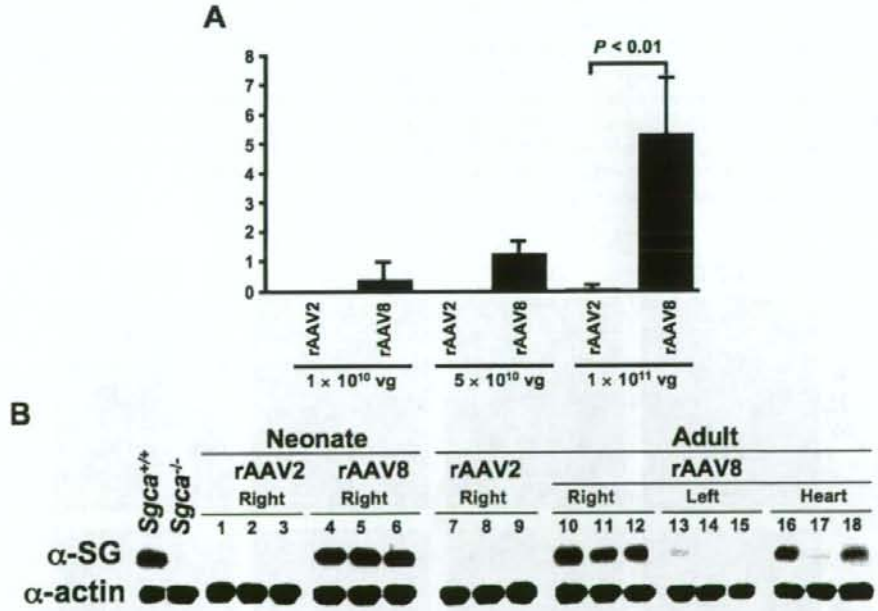

FIG. 3. Immunoblot analysis of α-SG in rAAV-injected α-SG-deficient muscles. Expression of α-SG in the hind limb muscles and heart of Sgca$^{-/-}$ mice was examined 4 weeks after rAAV injection, by real-time PCR and Western blot. (**A**) Real-time PCR was performed in duplicate to quantitate transgene copy number in each hind limb muscle after a single intramuscular administration of rAAV2-α-SG and rAAV8-α-SG. The right TA muscle of neonatal Sgca$^{-/-}$ mice was transduced with vector at 1×10^{10}, 5×10^{10}, and 1×10^{11} VG. Results are represented as vector copy number per diploid genome together with standard errors of mean. p Values are indicated and show a significant difference between rAAV2- and rAAV8-injected Sgca$^{-/-}$ mice ($p < 0.001$). (**B**) The right TA muscles of Sgca$^{-/-}$ mice were transduced with 1×10^{11} VG (neonates) or 5×10^{11} VG (adults) of rAAV2-α-SG (lanes 1–3 and 7–9) or rAAV8-α-SG (lanes 4–6 and 10–18). Ten-microgram samples of muscle lysates were separated by 10% SDS–PAGE. Faint bands were detected in the contralateral hind limb muscles of rAAV8-α-SG-injected mice. Adult Sgca$^{+/+}$ and Sgca$^{-/-}$ hind limb muscle lysates were used as positive and negative controls, respectively. The α-SG antibody detected a 50-kDa band. α-Sarcomeric actin is shown as a loading control.

tamyl transpeptidase (γ-GTP), albumin (ALB), and total protein (TP) in rAAV2-α-SG- and rAAV8-α-SG-injected Sgca$^{-/-}$ mice. Because skeletal muscle contains isozymes of creatine kinase, lactate dehydrogenase, aspartate aminotransferase, and ALT, these may be released into the blood stream after muscle necrosis (Janssen *et al.*, 1989); the ALT level in Sgca$^{-/-}$ mice was 5.4-fold higher than that in Sgca$^{+/+}$ mice ($p < 0.001$; Table 1). The ALT level in rAAV8-injected Sgca$^{-/-}$ mice was slightly lower than that in Sgca$^{-/-}$ mice. The levels of other liver-related proteins, including γ-GTP, ALB, and TP, were not significantly different between Sgca$^{-/-}$ and rAAV2-α-SG- and rAAV8-α-SG-injected Sgca$^{-/-}$ mice.

Tropism of rAAV2- and rAAV8-α-SG in α-SG-deficient mice

To investigate whether there is any difference in tissue tropism between rAAV2 and rAAV8, we determined the vector copies per diploid genome (C/DG) between the two vectors in injected skeletal muscle by a quantitative, real-time PCR assay. We injected neonatal Sgca$^{-/-}$ mice with either rAAV2-α-SG or rAAV8-α-SG at three different doses (1×10^{10}, 5×10^{10}, or 1×10^{11} VG/mouse) via the TA muscle ($n = 3$ per group). At a dose of 1×10^{11} VG/mouse, we detected rAAV2-α-SG and rAAV8-α-SG vector genomes in skeletal muscle at levels of 0.05 ± 0.03 and 5.33 ± 1.88 C/DG, respectively ($p < 0.01$; Fig. 3A). Increasing doses of rAAV8-α-SG resulted in increased levels of transgene expression. Higher transduction efficiency was observed with rAAV8-α-SG when large amounts of vector were used. Moreover, to evaluate the amount of α-SG in rAAV2-α-SG- or rAAV8-α-SG-injected skeletal muscles of Sgca$^{-/-}$ mice, we performed Western blot analysis. Four weeks after injection of rAAV2-α-SG into the TA muscle of neonatal and adult Sgca$^{-/-}$ mice, α-SG was almost undetectable (Fig. 3B). In contrast, when rAAV8-α-SG was injected into the right TA muscle of neonatal Sgca$^{-/-}$ mice, the amount of α-SG in rAAV8-transduced muscles was 3.5-fold higher than that in Sgca$^{+/+}$ muscles. When transduced in adulthood, the expression level of α-SG in the TA muscle of Sgca$^{-/-}$ mice was almost equal to that in Sgca$^{+/+}$ muscle. In addition, α-SG was detected in contralateral hind limb muscles and the heart after injection of rAAV8-α-SG into the TA muscle (Fig. 3B).

rAAV8-mediated α-SG expression ameliorated muscle pathology

A defect in any one of the four SGs can disrupt the entire SG complex in LGMD 2C-2F patients. Thus, we investigated the presence of a SG complex in the sarcolemma 4 weeks after injection of rAAV8-α-SG into the TA muscle of neonatal Sgca$^{-/-}$ mice. Immunostaining of rAAV8-α-SG-injected TA muscle with anti-SGs antibodies revealed that restoration of α-SG expression accompanied the sarcolemmal expression of other components of the SG complex, that is, β-, γ-, and δ-SG (Fig. 4). Moreover, 4 weeks after rAAV8-α-SG injection, H&E staining demonstrated considerable amelioration of the muscle pathology of rAAV8-injected TA muscles (Fig. 5A), and of surrounding EDL, SOL, GAS, and TP/PL muscles (data not shown). In contrast, uninjected and rAAV2-α-SG-injected muscles of Sgca$^{-/-}$ mice still showed signs of muscle degeneration and regeneration. To evaluate the amelioration of the dystrophic phenotype (Morgan *et al.*, 1990; Duclos *et al.*, 1998; Li *et al.*, 1999; Allamand *et al.*, 2000; Dressman *et al.*, 2002), we counted centrally nucleated myofibers in rAAV8-α-SG-injected muscles 4 months after injection (Fig. 5B). Sgca$^{-/-}$ hind limb muscles showed approximately 90% centrally nucleated myofibers. In contrast, rAAV8-α-SG-injected TA and ipsilateral EDL and SOL muscles showed

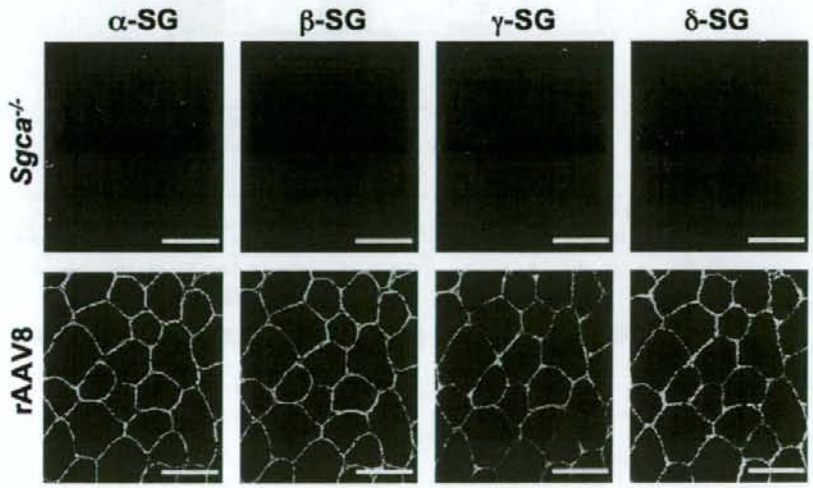

FIG. 4. Complete restoration of sarcoglycan expression at the sarcolemma of α-SG-deficient muscle after rAAV8-α-SG injection. Right TA muscles of neonatal Sgca$^{-/-}$ mice were injected with 1×10^{11} VG of rAAV8-α-SG. Untreated and rAAV8-injected Sgca$^{-/-}$ TA muscles (*top* and *bottom*, respectively) were labeled by indirect immunofluorescence, using specific antibodies against β-SG, γ-SG, or δ-SG. Untreated Sgca$^{-/-}$ muscle showed a secondary loss of SGs from the sarcolemma. Four weeks after injection, SGs were expressed in rAAV8-injected Sgca$^{-/-}$ muscle. Scale bars: 50 μm.

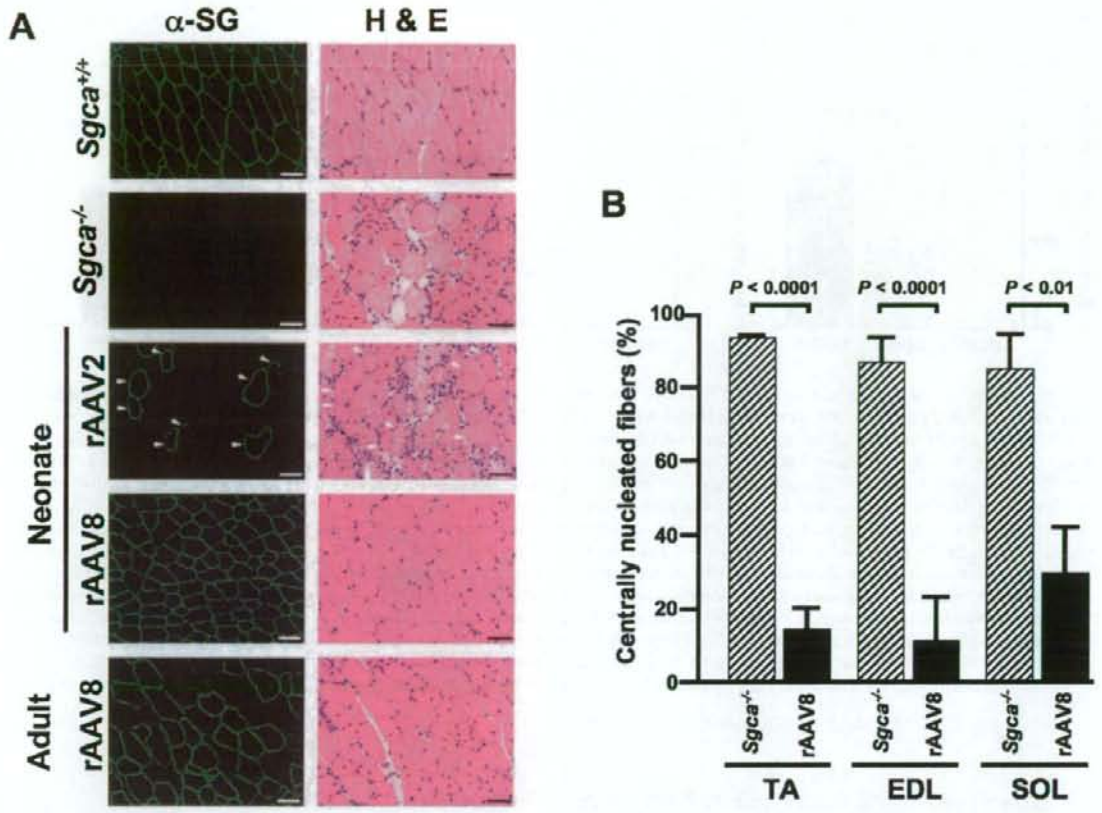

FIG. 5. Reduction of muscle degeneration in α-SG-deficient mice after rAAV8-α-SG-mediated gene transfer. (**A**) Right TA muscles of neonatal or adult Sgca$^{-/-}$ mice were transduced with 1×10^{11} VG (neonates) or 5×10^{11} VG (adults) of rAAV2-α-SG or rAAV8-α-SG. Four weeks after rAAV injection, serial cross-sections of Sgca$^{+/+}$, Sgca$^{-/-}$, and rAAV2- or rAAV8-injected Sgca$^{-/-}$ TA muscles (rAAV2 and rAAV8, respectively) were labeled by indirect immunofluorescence, using α-SG antibody (*left*, green), and stained with hematoxylin and eosin (H&E) (*right*). rAAV8-injected Sgca$^{-/-}$ TA muscles showed no signs of muscle degeneration. Arrowheads indicate α-SG-positive fibers. Scale bars: 50 μm. (**B**) Percentages of centrally nucleated myofibers in Sgca$^{-/-}$ skeletal muscles 4 months after injection of rAAV8-α-SG. Right TA muscles of neonatal Sgca$^{-/-}$ mice were transduced with 1×10^{11} VG of rAAV8-α-SG. Centrally nucleated myofibers among more than 200 total myofibers were counted in randomly selected H&E-stained cross-sections of the hind limb from Sgca$^{-/-}$ mice (hatched columns) and rAAV8-α-SG-injected Sgca$^{-/-}$ mice (solid columns) ($n = 3$ for each group). The percentage of centrally nucleated myofibers in rAAV8-α-SG-injected Sgca$^{-/-}$ mice was significantly lower than that in untreated Sgca$^{-/-}$ mice. p Values showed a statistically significant difference between Sgca$^{-/-}$ mice and rAAV8-injected Sgca$^{-/-}$ mice ($p < 0.0001$ for TA, $p < 0.0001$ for EDL, and $p < 0.01$ for SOL).

13.2 ± 7.3, 10.4 ± 10.4, and 29.1 ± 12.9% centrally nucleated myofibers, respectively ($p < 0.0001$, $p < 0.0001$, and $p < 0.0023$, respectively; Fig. 5B). The percentage of centrally nucleated myofibers in rAAV8-injected hind limb was significantly lower than that of Sgca$^{-/-}$ muscle, indicating that full recovery of the SG complex at the sarcolemma of Sgca$^{-/-}$ mice corrected the underlying biochemical deficiency and consequently restored the integrity of the muscle membrane.

rAAV-8-mediated α-SG expression improves contractile force and reverses muscle hypertrophy of α-SG-deficient muscle

A major functional deficit in muscular dystrophy patients is the loss of muscle strength. In our previous physiological study of muscular dystrophy model animals, we confirmed profound muscle force deficits in TA muscle (Yoshimura *et al.*, 2004; Imamura *et al.*, 2005).

A deficiency of α-SG decreases the contractile force of affected muscles (Danieli-Betto *et al.*, 2005; Imamura *et al.*, 2005). To evaluate whether rAAV8-α-SG transfer might improve Sgca$^{-/-}$ muscle physiological function, we measured the contractile force of rAAV8-injected Sgca$^{-/-}$ TA and EDL muscles. TA and EDL muscles were carefully separated from the hind limb and subjected to *in vitro* electrophysiological stimulation and contractile measurement on a force transducer. First, the right TA muscles of neonatal Sgca$^{-/-}$ mice were transduced with 1×10^{11} VG of rAAV8-α-SG. At the age of 5 months, the specific tetanic force of untreated Sgca$^{+/+}$ and Sgca$^{-/-}$ TA muscles was 17.3 ± 4.5 and 8.9 ±

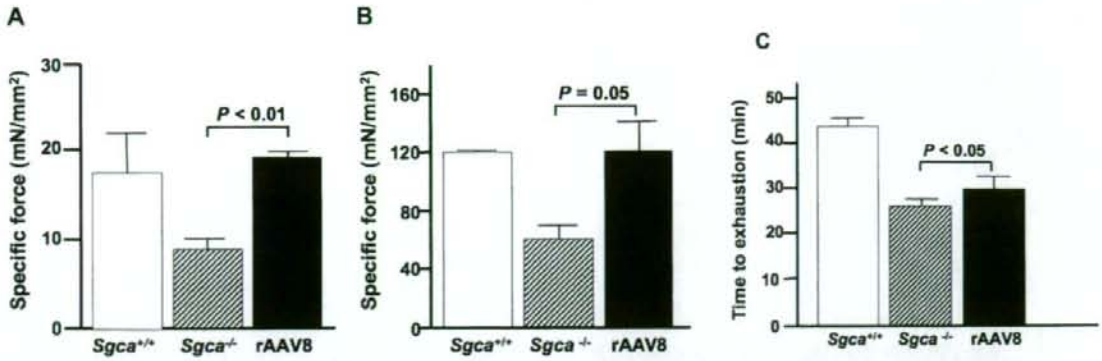

FIG. 6. Recovery of contractile force of α-SG-deficient muscle after transduction with rAAV8-α-SG. Right TA muscles of neonatal or adult $Sgca^{-/-}$ mice were transduced with 1×10^{11} VG (neonates) or 5×10^{11} VG (adults) of rAAV8-α-SG, and tetanic forces and time to exhaustion were assessed *in vitro* and *in vivo*. (**A**) Specific tetanic force of TA muscles from $Sgca^{+/+}$ (open column, $n = 3$), untreated $Sgca^{-/-}$ (hatched column, $n = 3$), and rAAV8-α-SG-injected $Sgca^{-/-}$ mice (solid column, $n = 3$). The right TA muscles of neonatal $Sgca^{-/-}$ mice were transduced with 1×10^{11} VG of rAAV8-α-SG, and the tetanic forces of TA muscles were assessed *in vitro* 5 months after injection. (**B**) Specific tetanic force of EDL muscles from $Sgca^{+/+}$ (open column, $n = 3$), untreated $Sgca^{-/-}$ (hatched column, $n = 3$), and rAAV8-α-SG-injected $Sgca^{-/-}$ mice (solid column, $n = 4$). The right TA muscles of adult $Sgca^{-/-}$ mice were transduced with 5×10^{11} VG of rAAV8-α-SG, and the tetanic forces of EDL muscles were assessed *in vitro* 10 weeks after injection. The p values show a statistically significant difference between $Sgca^{-/-}$ mice and rAAV8-injected $Sgca^{-/-}$ mice ($p < 0.01$ for TA, and $p = 0.05$ for EDL). (**C**) Time to exhaustion in treadmill test: $Sgca^{+/+}$ (open column, $n = 3$), untreated $Sgca^{-/-}$ (hatched column, $n = 4$), and rAAV8-α-SG-injected $Sgca^{-/-}$ mice (solid column, $n = 4$). The right TA muscles of adult $Sgca^{-/-}$ mice were transduced with 5×10^{11} VG of rAAV8-α-SG, and the tetanic forces of EDL muscles were assessed *in vitro* 10 weeks after injection. The p values show a statistically significant difference between $Sgca^{-/-}$ mice and rAAV8-injected $Sgca^{-/-}$ mice ($p < 0.05$).

1.2 mN/mm², respectively, whereas that of rAAV8-injected $Sgca^{-/-}$ TA muscle was 19.4 ± 0.7 mN/mm² ($p < 0.01$; Fig. 6A and Table 2). Furthermore, we assessed the improvement of EDL muscle after rAAV8-α-SG injection in adulthood. rAAV8-α-SG (5×10^{11} VG) was injected into the right TA muscle of adult $Sgca^{-/-}$ mice. We measured the contractile force of the EDL muscle surrounding rAAV8-injected TA muscle 10 weeks after injection. The specific tetanic forces of $Sgca^{+/+}$ and $Sgca^{-/-}$ EDL muscles were 121.5 ± 1.6 and 61.74 ± 8.33 mN/mm², and that of rAAV8-injected $Sgca^{-/-}$ EDL muscle was 121.15 ± 22.12 mN/mm² ($p = 0.05$; Fig. 6B and Table 2). Consequently, the specific tetanic force of animals injected with rAAV8-α-SG was 2-fold higher than that of uninjected $Sgca^{-/-}$ TA muscle ($p < 0.01$, and $p = 0.05$; Fig. 6A and B, Table 2).

In addition to the drastic improvement in contractile force of rAAV8-α-SG-injected TA muscle, the weight of rAAV8-α-SG-injected TA and EDL muscles as a percentage of body weight was comparable to those of $Sgca^{+/+}$ muscle and much smaller than those of their untreated counterparts (Table 2), suggesting that rAAV8-α-SG treatment reduced the muscle hypertrophy of $Sgca^{-/-}$ muscle. Moreover, we investigated whether α-SG expression in $Sgca^{-/-}$ muscle effectively increases the physical performance of the muscle. In an enforced treadmill test, the exhaustion times of $Sgca^{-/-}$ and rAAV8-α-SG injected $Sgca^{-/-}$ mice were 25.9 ± 2.0 and 30 ± 2.6 min ($p < 0.05$; Fig. 6C). rAAV8-injected $Sgca^{-/-}$ mice demonstrated increased exercise time before reaching exhaustion and could run longer distances.

Discussion

In this paper, we have presented evidence that a single intramuscular injection of a rAAV8 vector expressing human α-SG cDNA via a CMV promoter could achieve efficient therapeutic effects in a dystrophic animal model of LGMD 2D.

When rAAV8-α-SG was administered to neonatal $Sgac^{-/-}$ mice, we observed extensive α-SG transduction in the hind limb muscles, including the TA, EDL, SOL, and GAS muscles. In the case of rAAV8 injection of adult $Sgac^{-/-}$ mice, α-SG was expressed not only in all of the hind limb muscles and but also in cardiac muscle. A similar profile was further confirmed in a study by Wang and coworkers, in which they delivered more potent double-stranded rAAV8 vectors into adult and neonatal mice. The rAAV8 vector is more stable in the bloodstream than other rAAV serotypes when administered intravascularly and extravascularly (Wang *et al.*, 2005). The 37/67-kDa laminin receptor (LamR) has been identified as the host cell receptor for the AAV8 vector (Akache *et al.*, 2006). LamR is widely expressed in human tissues, where it is normally involved in interactions of extracellular laminin-1 with proteases and the cell (Ardini *et al.*, 1997, 2002). Furthermore, the rAAV8 vector might be able to cross the capillary endothelial cell barrier and transduce remote organs with high efficiency (Inagaki *et al.*, 2006). However, the detailed mechanism of rAAV8-mediated cell recognition and transduction has yet to be fully elucidated.

In the present study, we demonstrated that rAAV8-α-SG transduced skeletal muscle about 100-fold more compared with rAAV2-α-SG. In addition, rAAV8-α-SG-injected

TABLE 2. CONTRACTILE PROPERTIES OF rAAV8-INJECTED α-SARCOGLYCAN DEFICIENT MUSCLE[a,b]

	Injection age	*Number of mice*	*Tissue*	*Muscle length (L_o, mm)*	*Muscle weight (mg)*	*Tissue weight (% of body weight)*	*CSA (mm^2)*	*Maximal contraction (P_o, mN)*	*Specific force (mN/mm^2)*
$Sgca^{+/+}$	10-day-old	3	TA	11	56.1 ± 2.9	0.185 ± 0.004	4.81 ± 0.14	82.3 ± 19.2	17.3 ± 4.5
$Sgca^{-/-}$	10-day-old	3	TA	11.5	68.1 ± 6.9	0.233 ± 0.023	5.61 ± 0.32	48.5 ± 4.0	8.9 ± 1.2
rAAV8-injected $Sgca^{-/-}$	10-day-old	3	TA	11.5	65.7 ± 8.2	0.224 ± 0.027	5.05 ± 0.46	103.8 ± 10.3	19.4 ± 0.7[c]
$Sgca^{+/+}$	7-week-old	3	EDL	14.83 ± 0.83	11.30 ± 0.46	0.044 ± 0.001	0.73 ± 0.07	88.3 ± 8.5	121.5 ± 1.6
$Sgca^{-/-}$	7-week-old	3	EDL	14	13.5 ± 0.48	0.047 ± 0.002	0.91 ± 0.03	56.94 ± 9.25	61.74 ± 8.33
rAAV8-Injected $Sgca^{-/-}$	7-week-old	4	EDL	14	10.7 ± 0.84	0.038 ± 0.003	0.72 ± 0.06[d]	84.04 ± 8.74	121.15 ± 22.12[e]

Abbreviations: CSA, tissue cross-sectional area; EDL, extensor digitorum longus; TA, tibialis anterior.
[a]Data represent means ± SE. Tissue weights were normalized to respective body weights.
[b]The p values indicate statistical significance between $Sgca^{-/-}$ mice and rAAV8-injected $Sgca^{-/-}$ mice.
[c]$p < 0.01$ when rAAV8 was injected into neonatal $Sgca^{-/-}$ TA muscle.
[d]$p \leq 0.05$ when rAAV8 was injected into adult $Sgca^{-/-}$ EDL muscle.
[e]$p \leq 0.05$ when rAAV8 was injected into adult $Sgca^{-/-}$ EDL muscle.

Sgca$^{-/-}$ mice did not demonstrate cytotoxic and immunological reactions for more than 7 months after injection. Transduction of α-SG in an LGMD 2D animal model by means of adenovirus, rAAV1, or rAAV2 vector was previously reported (Duclos *et al.*, 1998; Allamand *et al.*, 2000; Dressman *et al.*, 2002; Fougerousse *et al.*, 2007; Pacak *et al.*, 2007). In the two studies using the adenovirus vector, it was necessary to use neonatal animals to take advantage of the immaturity of the immune system and thereby to circumvent the strong immune response elicited by the adenoviral vector (Duclos *et al.*, 1998; Allamand *et al.*, 2000). The AAV vector, which has been more widely used, is nonpathogenic, has low immunogenicity, and has been shown to confer long-term gene expression in muscles of various species. Use of the ubiquitous CMV promoter would allow expression of the transgene in various cells. Therefore, expression of α-SG via rAAV1 and rAAV2, using the CMV promoter, induced an immune response, whereas those vectors introduced balanced expression of SGs within the injected Sgca$^{-/-}$ myofibers (Duclos *et al.*, 1998; Allamand *et al.*, 2000; Dressman *et al.*, 2002; Fougerousse *et al.*, 2007; Pacak *et al.*, 2007). Between 28 and 41 days after rAAV2 injection, a drastic decrease in α-SG expression occurred in the injected Sgca$^{-/-}$ muscle. In particular, numerous antigen-presenting cells in the dystrophic muscles could direct a strong immune response against the transgene product when the CMV promoter was used (Yuasa *et al.*, 2002). On the other hand, the AAV8 vector transduced antigen-presenting cells (such as dendritic cells) less efficiently than did the rAAV2 vector (Xin *et al.*, 2006). Consequently, gene transduction via the AAV2 vector with the CMV promoter might be less efficient than with rAAV8 and other AAV serotypes.

Because the CMV promoter elicits an immune response against the transgene product (Cordier *et al.*, 2001; Yuasa *et al.*, 2002; Liu *et al.*, 2004), several studies of rAAV-mediated transduction of striated musculature used the muscle creatine kinase (MCK), CK6, or SP6 promoter as a muscle-specific promoter (Gregorevic *et al.*, 2004; Yoshimura *et al.*, 2004; Zhu *et al.*, 2005). Transduction driven by a muscle-specific promoter was achieved without acute toxicological response. Moreover, to enable strong expression in striated muscle, another group created a hybrid promoter containing the MCK enhancer and the simian virus 40 promoter (MCK/SV40 promoter) (Takeshita *et al.*, 2007). The MCK/SV40 promoter yielded long-term (>6 months) expression of a human secretory alkaline phosphatase (huSEAP) reporter gene after electrotransfer of the plasmid into mice. In addition, selection of the rAAV serotype is important. rAAV9 has also been shown to be efficient in cardiac or skeletal muscle transduction (Inagaki *et al.*, 2006; Sarkar *et al.*, 2006).

Our study demonstrated improvement of the contractile force and decreased sensitivity to stretch and exhaustion time for exercise in Sgca$^{-/-}$ muscle after rAAV8-α-SG injection. Recovery of absolute maximal force and specific tetanic force is one of the barometers of amelioration. A dose of about 1×10^{11} VG (for neonates) or 5×10^{11} VG (for adults) in Sgca$^{-/-}$ TA muscle led to transduction of approximately >70% of hind limb muscles and was sufficient to increase the global force of the animal. We compared tetanic contractions of rAAV8-α-SG-injected muscles with those of Sgca$^{+/+}$ and Sgca$^{-/-}$ muscles. The contractile forces of rAAV8-injected Sgca$^{-/-}$ TA and EDL muscles were increased 2-fold compared with that of Sgca$^{-/-}$ muscles. Furthermore, the exercise treadmill test results for rAAV8-injected Sgca$^{-/-}$ mice were higher than those of Sgca$^{-/-}$ mice. This suggested that increased synthesis of α-SG had no adverse effects on SG complex formation, and that overexpression of α-SG might induce stability of the transmembrane without causing muscle pathology. In a therapeutic study using rAAV1 (Fougerousse *et al.*, 2007), injection of rAAV1 encoding α-SG cDNA via the C5-12 promoter (a muscle-specific promoter) into the artery of Sgca$^{-/-}$ mice increased the contractile force of EDL muscles 1.5-fold compared with that of Sgca$^{-/-}$ EDL muscles. Therefore, rAAV8 would be an effective tool for the delivery of therapeutic genes to skeletal muscles in the treatment of limb-girdle muscular dystrophy.

Acknowledgments

The authors greatly appreciate the technical support and helpful discussion provided by Ms. Kazue Kinoshita and Dr. Katsutoshi Yuasa. We thank Dr. Eva Engvall for providing the Sgca$^{-/-}$ mice. This work was supported by a Grant for Research on Nervous and Mental Disorders (16B-2) and by Health Science Research Grants for Research on the Human Genome and Gene Therapy (H16-genome-003) and for Research on Brain Science (H15-kokoro-021 and H18-kokoro-019) from the Ministry of Health, Labor, and Welfare; and by Grants in Aid for Scientific Research (16390418, 16590333, 18590392, and 19390383) from the Ministry of Education, Culture, Sports, Science, and Technology.

References

Akache, B., Grimm, D., Pandey, K., Yant, S.R., Xu, H., and Kay, M.A. (2006). The 37/67-kilodalton laminin receptor is a receptor for adeno-associated virus serotypes 8, 2, 3, and 9. J. Virol. 80, 9831–9836.

Allamand, V., Donahue, K.M., Straub, V., Davisson, R.L., Davidson, B.L., and Campbell, K.P. (2000). Early adenovirus-mediated gene transfer effectively prevents muscular dystrophy in α-sarcoglycan-deficient mice. Gene Ther. 7, 1385–1391.

Araishi, K., Sasaoka, T., Imamura, M., Noguchi, S., Hama, H., Wakabayashi, E., Yoshida, M., Hori, T., and Ozawa, E. (1999). Loss of the sarcoglycan complex and sarcospan leads to muscular dystrophy in β-sarcoglycan-deficient mice. Hum. Mol. Genet. 8, 1589–1598.

Ardini, E., Tagliabue, E., Magnifico, A., Buto, S., Castronovo, V., Colnaghi, M.I., and Menard, S. (1997). Co-regulation and physical association of the 67-kDa monomeric laminin receptor and the $\alpha_6\beta_4$ integrin. J. Biol. Chem. 272, 2342–2345.

Ardini, E., Sporchia, B., Pollegioni, L., Modugno, M., Ghirelli, C., Castiglioni, F., Tagliabue, E., and Menard, S. (2002). Identification of a novel function for 67-kDa laminin receptor: Increase in laminin degradation rate and release of motility fragments. Cancer Res. 62, 1321–1325.

Bonnemann, C.G., Modi, R., Noguchi, S., Mizuno, Y., Yoshida, M., Gussoni, E., McNally, E.M., Duggan, D.J., Angelini, C., and Hoffman, E.P. (1995). β-Sarcoglycan (A3b) mutations cause autosomal recessive muscular dystrophy with loss of the sarcoglycan complex. Nat. Genet. 11, 266–273.

Burton, M., Nakai, H., Colosi, P., Cunningham, J., Mitchell, R., and Couto, L. (1999). Coexpression of factor VIII heavy and light chain adeno-associated viral vectors produces biologically active protein. Proc. Natl. Acad. Sci. U.S.A. 96, 12725–12730.

Cordier, L., Gao, G.P., Hack, A.A., McNally, E.M., Wilson, J.M., Chirmule, N., and Sweeney, H.L. (2001). Muscle-specific promoters may be necessary for adeno-associated virus-mediated gene transfer in the treatment of muscular dystrophies. Hum. Gene Ther. 12, 205–215.

Danieli-Betto, D., Esposito, A., Germinario, E., Sandona, D., Martinello, T., Jakubiec-Puka, A., Biral, D., and Betto, R. (2005). Deficiency of α-sarcoglycan differently affects fast- and slow-twitch skeletal muscles. Am. J. Physiol. Regul. Integr. Comp. Physiol. 289, R1328–R1337.

Dressman, D., Araishi, K., Imamura, M., Sasaoka, T., Liu, L.A., Engvall, E., and Hoffman, E.P. (2002). Delivery of α- and β-sarcoglycan by recombinant adeno-associated virus: Efficient rescue of muscle, but differential toxicity. Hum. Gene Ther. 13, 1631–1646.

Duclos, F., Straub, V., Moore, S.A., Venzke, D.P., Hrstka, R.F., Crosbie, R.H., Durbeej, M., Lebakken, C.S., Ettinger, A.J., Van Der Meulen, J., Holt, K.H., Lim, L.E., Sanes, J.R., Davidson, B.L., Faulkner, J.A., Williamson, R., and Campbell, K.P. (1998). Progressive muscular dystrophy in α-sarcoglycan-deficient mice. J. Cell Biol. 142, 1461–1471.

Ervasti, J.M., Ohlendieck, K., Kahl, S.D., Gaver, M.G., and Campbell, K.P. (1990). Deficiency of a glycoprotein component of the dystrophin complex in dystrophic muscle. Nature 345, 315–319.

Eymard, B., Romero, N.B., Leturcq, F., Piccolo, F., Carrie, A., Jeanpierre, M., Collin, H., Deburgrave, N., Azibi, K., Chaouch, M., Merlini, L., Themar-Noel, C., Penisson, I., Mayer, M., Tanguy, O., Campbell, K.P., Kaplan, J.C., Tome, F.M., and Fardeau, M. (1997). Primary adhalinopathy (α-sarcoglycanopathy): Clinical, pathologic, and genetic correlation in 20 patients with autosomal recessive muscular dystrophy. Neurology 48, 1227–1234.

Fanin, M., Duggan, D.J., Mostacciuolo, M.L., Martinello, F., Freda, M.P., Soraru, G., Trevisan, C.P., Hoffman, E.P., and Angelini, C. (1997). Genetic epidemiology of muscular dystrophies resulting from sarcoglycan gene mutations. J. Med. Genet. 34, 973–977.

Fisher, K.J., Jooss, K., Alston, J., Yang, Y., Haecker, S.E., High, K., Pathak, R., Raper, S.E., and Wilson, J.M. (1997). Recombinant adeno-associated virus for muscle directed gene therapy. Nat. Med. 3, 306–312.

Fougerousse, F., Bartoli, M., Poupiot, J., Arandel, L., Durand, M., Guerchet, N., Gicquel, E., Danos, O., and Richard, I. (2007). Phenotypic correction of α-sarcoglycan deficiency by intra-arterial injection of a muscle-specific serotype 1 rAAV vector. Mol. Ther. 15, 53–61.

Gao, G., Vandenberghe, L.H., Alvira, M.R., Lu, Y., Calcedo, R., Zhou, X., and Wilson, J.M. (2004). Clades of adeno-associated viruses are widely disseminated in human tissues. J. Virol. 78, 6381–6388.

Gao, G.P., Alvira, M.R., Wang, L., Calcedo, R., Johnston, J., and Wilson, J.M. (2002). Novel adeno-associated viruses from rhesus monkeys as vectors for human gene therapy. Proc. Natl. Acad. Sci. U.S.A. 99, 11854–11859.

Greelish, J.P., SU, L.T., Lankford, E.B., Burkman, J.M., Chen, H., Konig, S.K., Mercier, I.M., Desjardins, P.R., Mitchell, M.A., Zheng, X.G., Leferovich, J., Gao, G.P., Balice-Gordon, R.J., Wilson, J.M., and Stedman, H.H. (1999). Stable restoration of the sarcoglycan complex in dystrophic muscle perfused with histamine and a recombinant adeno-associated viral vector. Nat. Med. 5, 439–443.

Gregorevic, P., Blankinship, M.J., Allen, J.M., Crawford, R.W., Meuse, L., Miller, D.G., Russell, D.W., and Chamberlain, J.S. (2004). Systemic delivery of genes to striated muscles using adeno-associated viral vectors. Nat. Med. 10, 828–834.

Imamura, M., Araishi, K., Noguchi, S., and Ozawa, E. (2000). A sarcoglycan–dystroglycan complex anchors Dp116 and utrophin in the peripheral nervous system. Hum. Mol. Genet. 9, 3091–3100.

Imamura, M., Mochizuki, Y., Engvall, E., and Takeda, S. (2005). ε-Sarcoglycan compensates for lack of α-sarcoglycan in a mouse model of limb-girdle muscular dystrophy. Hum. Mol. Genet. 14, 775–783.

Inagaki, K., Fuess, S., Storm, T.A., Gibson, G.A., McTiernan, C.F., Kay, M.A., Nakai, H., Sarkar, R., Mucci, M., Addya, S., Tetreault, R., Bellinger, D.A., Nichols, T.C., and Kazazian, H.H., Jr. (2006). Robust systemic transduction with AAV9 vectors in mice: Efficient global cardiac gene transfer superior to that of AAV8. Mol. Ther. 14, 45–53.

Iwata, Y., Nakamura, H., Mizuno, Y., Yoshida, M., Ozawa, E., and Shigekawa, M. (1993). Defective association of dystrophin with sarcolemmal glycoproteins in the cardiomyopathic hamster heart. FEBS Lett. 329, 227–231.

Janssen, G.M., Kuipers, H., Willems, G.M., Does, R.J., Janssen, M.P., and Geurten, P. (1989). Plasma activity of muscle enzymes: Quantification of skeletal muscle damage and relationship with metabolic variables. Int. J. Sports Med. 10(Suppl. 3), S160–S168.

Kessler, P.D., Podsakoff, G.M., Chen, X., McQuiston, S.A., Colosi, P.C., Matelis, L.A., Kurtzman, G.J., and Byrne, B.J. (1996). Gene delivery to skeletal muscle results in sustained expression and systemic delivery of a therapeutic protein. Proc. Natl. Acad. Sci. U.S.A. 93, 14082–14087.

Kyhse-Andersen, J. (1984). Electroblotting of multiple gels: A simple apparatus without buffer tank for rapid transfer of proteins from polyacrylamide to nitrocellulose. J. Biochem. Biophys. Methods 10, 203–209.

Laemmli, U.K. (1970). Cleavage of structural proteins during the assembly of the head of bacteriophage T4. Nature 227, 680–685.

Li, J., Dressman, D., Tsao, Y.P., Sakamoto, A., Hoffman, E.P., and Xiao, X. (1999). rAAV vector-mediated sarcoglycan gene transfer in a hamster model for limb girdle muscular dystrophy. Gene Ther. 6, 74–82.

Liu, Y.L., Mingozzi, F., Rodriguez-Colon, S.M., Joseph, S., Dobrzynski, E., Suzuki, T., High, K.A., and Herzog, R.W. (2004). Therapeutic levels of factor IX expression using a muscle-specific promoter and adeno-associated virus serotype 1 vector. Hum. Gene Ther. 15, 783–792.

McNally, E.M., Yoshida, M., Mizuno, Y., Ozawa, E., and Kunkel, L.M. (1994). Human adhalin is alternatively spliced and the gene is located on chromosome 17q21. Proc. Natl. Acad. Sci. U.S.A. 91, 9690–9694.

Morgan, J.E., Hoffman, E.P., and Partridge, T.A. (1990). Normal myogenic cells from newborn mice restore normal histology to degenerating muscles of the *mdx* mouse. J. Cell Biol. 111, 2437–2449.

Mourkioti, F., Kratsios, P., Luedde, T., Song, Y.H., Delafontaine, P., Adami, R., Parente, V., Bottinelli, R., Pasparakis, M., and Rosenthal, N. (2006). Targeted ablation of IKK2 improves skeletal muscle strength, maintains mass, and promotes regeneration. J. Clin. Invest. 116, 2945–2954.

Nigro, V., De Sa Moreira, E., Piluso, G., Vainzof, M., Belsito, A., Politano, L., Puca, A.A., Passos-Bueno, M.R., and Zatz, M. (1996). Autosomal recessive limb-girdle muscular dystrophy, LGMD2F, is caused by a mutation in the δ-sarcoglycan gene. Nat. Genet. 14, 195–198.

Noguchi, S., McNally, E.M., Ben Othmane, K., Hagiwara, Y., Mizuno, Y., Yoshida, M., Yamamoto, H., Bonnemann, C.G., Gussoni, E., Denton, P.H., Kyriakides, T., Middleton, L., Hen-

tati, F., Ben Hamida, M., Nonaka, I., Vance, J.M., Kunkel, L.M., and Ozawa, E. (1995). Mutations in the dystrophin-associated protein γ-sarcoglycan in chromosome 13 muscular dystrophy. Science 270, 819–822.

Noguchi, S., Wakabayashi, E., Imamura, M., Yoshida, M., and Ozawa, E. (1999). Developmental expression of sarcoglycan gene products in cultured myocytes. Biochem. Biophys. Res. Commun. 262, 88–93.

Pacak, C.A., Walter, G.A., Gaidosh, G., Bryant, N., Lewis, M.A., Germain, S., Mah, C.S., Campbell, K.P., and Byrne, B.J. (2007). Long-term skeletal muscle protection after gene transfer in a mouse model of LGMD-2D. Mol. Ther. 15, 1775–1781.

Sarkar, R., Mucci, M., Addya, S., Tetreault, R., Bellinger, D.A., Nichols, T.C., and Kazazian, H.H., Jr. (2006). Long-term efficacy of adeno-associated virus serotypes 8 and 9 in hemophilia a dogs and mice. Hum. Gene Ther. 17, 427–439.

Takeshita, F., Takase, K., Tozuka, M., Saha, S., Okuda, K., Ishii, N., and Sasaki, S. (2007). Muscle creatine kinase/SV40 hybrid promoter for muscle-targeted long-term transgene expression. Int. J. Mol. Med. 19, 309–315.

Wang, Z., Zhu, T., Qiao, C., Zhou, L., Wang, B., Zhang, J., Chen, C., Li, J., and Xiao, X. (2005). Adeno-associated virus serotype 8 efficiently delivers genes to muscle and heart. Nat. Biotechnol. 23, 321–328.

Wigler, M., Perucho, M., Kurtz, D., Dana, S., Pellicer, A., Axel, R., and Silverstein, S. (1980). Transformation of mammalian cells with an amplifiable dominant-acting gene. Proc. Natl. Acad. Sci. U.S.A. 77, 3567–3570.

Xiao, X., Li, J., and Samulski, R.J. (1996). Efficient long-term gene transfer into muscle tissue of immunocompetent mice by adeno-associated virus vector. J. Virol. 70, 8098–8108.

Xiao, X., Li, J., and Samulski, R.J. (1998). Production of high-titer recombinant adeno-associated virus vectors in the absence of helper adenovirus. J. Virol. 72, 2224–2232.

Xiao, X., Li, J., Tsao, Y.P., Dressman, D., Hoffman, E.P., and Watchko, J.F. (2000). Full functional rescue of a complete muscle (TA) in dystrophic hamsters by adeno-associated virus vector-directed gene therapy. J. Virol. 74, 1436–1442.

Xin, K.Q., Mizukami, H., Urabe, M., Toda, Y., Shinoda, K., Yoshida, A., Oomura, K., Kojima, Y., Ichino, M., Klinman, D., Ozawa, K., and Okuda, K. (2006). Induction of robust immune responses against human immunodeficiency virus is supported by the inherent tropism of adeno-associated virus type 5 for dendritic cells. J. Virol. 80, 11899–11910.

Yamamoto, H., Mizuno, Y., Hayashi, K., Nonaka, I., Yoshida, M., and Ozawa, E. (1994). Expression of dystrophin-associated protein 35DAG (A4) and 50DAG (A2) is confined to striated muscles. J. Biochem. 115, 162–167.

Yoshida, M., and Ozawa, E. (1990). Glycoprotein complex anchoring dystrophin to sarcolemma. J. Biochem. 108, 748–752.

Yoshimura, M., Sakamoto, M., Ikemoto, M., Mochizuki, Y., Yuasa, K., Miyagoe-Suzuki, Y., and Takeda, S. (2004). AAV vector-mediated microdystrophin expression in a relatively small percentage of *mdx* myofibers improved the *mdx* phenotype. Mol. Ther. 10, 821–828.

Yuasa, K., Sakamoto, M., Miyagoe-Suzuki, Y., Tanouchi, A., Yamamoto, H., Li, J., Chamberlain, J.S., Xiao, X., and Takeda, S. (2002). Adeno-associated virus vector-mediated gene transfer into dystrophin-deficient skeletal muscles evokes enhanced immune response against the transgene product. Gene Ther. 9, 1576–1588.

Zhu, T., Zhou, L., Mori, S., Wang, Z., McTiernan, C.F., Qiao, C., Chen, C., Wang, D.W., Li, J., and Xiao, X. (2005). Sustained whole-body functional rescue in congestive heart failure and muscular dystrophy hamsters by systemic gene transfer. Circulation 112, 2650–2659.

Address reprint requests to:
Dr. Shin'ichi Takeda or Dr. Takashi Okada
Department of Molecular Therapy
National Institute of Neuroscience, NCNP
4-1-1 Ogawa-higashi, Kodaira
Tokyo 187-8502, Japan

E-mail: takeda@ncnp.go.jp or t-okada@ncnp.go.jp

Received for publication January 4, 2008; accepted after revision May 14, 2008.

Published online: June 17, 2008.